NUMERICAL INVESTIGATION OF MAGNETO-HYDRODYNAMIC FLOW WITH VARIABLE FLUID VISCOSITY AND HEAT TRANSFER IN PRESENCE OF SYMMETRICAL POROUS WEDGE

Santosh Kumar Dixit[1], Ramesh Yadav[2*] & Navneet Kumar Singh[3]

[1]Department of Mathematics, SGT University, Gurgaon, India

[2]Department of Mathematics, Babu Banarasi Das National Institute of Technology and Management, Lucknow U. P. India

[3]Department of Mathematics, Babu Banarasi Das Northern India Institute of Technology, Lucknow, U.P. India

[*]Corresponding author E. Mail. I.D: rky. pcm@gmail.com

ABSTRACT:

The numerical investigation of magneto-hydro-dynamic fluid with variable fluid viscosity and heat transfer in the presence of symmetrical porous wedge has been studied. The non-linear differential equations are solved numerically using MATLAB software with the help of ode45 solver. The main objective of this study is to investigate the effects of Hartmann Number M on the velocity and heat transfer of fluid and other effects such as Prandtl number Pr. Radiative heating parameter Q, Porous wedge parameter σ, Fluid viscosity variation parameter A, Falkner skan exponent m has been also seen graphically.

KEY WORDS: Porous wedge, Newtonian fluid, Prandtl number Pr, Radiative heating parameter(Q), Hartmann number M.

NOMENCLATURE

A	Fluid viscosity variation parameter	Pr	Prandtl number
C_p	Specific heat	Q	Radiative heating parameter
F	Non dimensional stream function	q_r	Radiative heat flux
$k*$	Absorption coefficient	T, T_w, T_∞	Temperature of the fluid, wall, free stream
m	Falkner-Skan exponent		

Greek symbols

α, γ	Transformation parameters	ν	Reference kinematic viscosity
λ	Similarity variable	ψ	Stream function
κ	Thermal conductivity	σ_s	Stefan-Boltzmann constant
μ, μ^*	Dynamic, reference viscosity	ρ	Density of the fluid

θ	Non dimensional temperature	σ	Porous Parameter (Dimensionless)

1. INTRODUCTION

The thermal radiation effects may play important role in the controlling of the heat flow in the polymerization process in industry where the quality of the final product depends on the heat controlling factors to some extent such as high temperature plasmas, liquid metal fluids, power generation systems are some important applications of radiative heat transfer from a wall to conductive gray fluids. The MHD flow of fluid and heat transfer along a symmetrical wedge has gained considerable attention due to its vast applications in industry such as chemicals, cosmetics, pharmaceutical and its important bearings on several technological and natural processes. Hossain et al. (2000) have investigated Flow of viscous incompressible fluid with temperature dependent viscosity and thermal conductivity past a permeable wedge with uniform surface heat slux. Abd-el-Malek et al. (2002) have analyzed the solution of the Rayleigh problem for a power law non-Newtonian conducting fluid via group method. Hossain et al. (2006) have investigated unsteady mixed-convection boundary layer flow along a symmetric wedge with variable surface temperature.

Ganji and Rajabi (2006) have been studied assessment of homotopy-perturbation and perturbation methods in heat radiation equations. Daniels (2007) has investigated on the boundary layer structure of differentially heated cavity flow in a stably stratified porous medium. Mukhopadhyay (2009) has been studied the effect of radiation and variable fluid viscosity on flow and heat transfer along a symmetric wedge. Suratiand and Timol (2010) have analyzed numerical study of forced convection wedge flow of some non-Newtonian fluids. Ramesh Yadav et al. (2016) have been also investigated Numerical analysis of magneto-hydrodynamic flow with one porous bounding wall. Ramesh Yadav and Vivek Joseph (2016) have been studied numerical analysis of magneto-hydrodynamic flow of fluid with one porous bounding wall. They have been obtained effects of magnetic parameter M, Reynolds number Re and slip coefficient on velocity component of fluids in a channel flow. Ramesh Yadav and Navneet Kumar Singh (2017) have been studied analytical investigation of thermal radiation effects on laminar flow of fluid and heat transfer in a channel with two porous bounding walls on different permeability and in another paper Navneet Kumar Singh and Ramesh Yadav (2017) have bee analyzed the investigation of heat transfer of non-Newtonian fluid in the presence of a porous wall.

In this paper we have solve the non-linear differential equation by numerically using MATLAB software ode 45 solver. The effect of the temperature-dependent fluid viscosity parameter, Porous wedge parameter, Hartmann number, radiation parameter and the influence of Prandtl number on temperature fields on the flow of fluid has been investigated and analyzed with graphically.

2. MATHEMATICAL FORMULATION

Let us assume the steady flow, two dimensional, laminar boundary-layer flow of viscous incompressible non-Newtonian past a symmetrical sharp porous wedge with velocity given by $\bar{u}_e(\bar{x}) = U_\infty \left(\frac{\bar{x}}{L}\right)^m \; for \;\; m \leq 1$ where L is the characteristic length and m is the velocity exponent related to the included angle $\pi\beta \; by \, m = \frac{\beta}{2-\beta}$. For $m < 0$, the solution becomes singular at $\bar{x} = 0$, while for $m \geq 0$, the solution can be defined for all values of $\bar{x}$. The governing equations of such type of flow are, in the usual notations.

$$\frac{\partial \bar{u}}{\partial \bar{x}} + \frac{\partial \bar{v}}{\partial \bar{y}} = 0, \quad (1)$$

$$\bar{u}\frac{\partial \bar{u}}{\partial \bar{x}} + \bar{v}\frac{\partial \bar{u}}{\partial \bar{y}} = \bar{u}_e\frac{\partial \bar{u}_e}{\partial \bar{x}} + \frac{1}{\rho}\frac{\partial \mu}{\partial T}\frac{\partial T}{\partial \bar{y}}\frac{\partial \bar{u}}{\partial \bar{y}} + \frac{\mu}{\rho}\frac{\partial^2 \bar{u}}{\partial \bar{y}^2} - \frac{\mu'}{\rho k}\,\bar{u} - \frac{\sigma_e B_0^2}{\rho}\bar{u} \;, \quad (2)$$

$$\bar{u}\frac{\partial T}{\partial \bar{x}} + \bar{v}\frac{\partial T}{\partial \bar{y}} = \frac{k}{\rho C_p}\frac{\partial^2 T}{\partial \bar{y}^2} - \frac{1}{\rho C_p}\frac{\partial q_r}{\partial \bar{y}} \;, \quad (3)$$

where μ is dynamic viscosity of the fluid. The viscous dissipation term in the energy equation is neglected. $\bar{u}$ is the velocity of the fluid in $\bar{x}$ – direction, $and\; \bar{v}$ is the velocity of the fluid and $\bar{y}$ -directions.

Brewster 1972 has given the approximation for radiation, we can write it

$$q_r = -\frac{4\sigma_s}{3k^*}\frac{\partial T^4}{\partial \bar{y}} \;. \quad (4)$$

Let us assume the temperature difference within the flow of fluid is such that T^4 expanded in the form of Taylor series about T_∞ and neglecting higher orders terms, we get $T^4 \equiv 4T_\infty^3 T - 3T_\infty^4$. Then the equation (3) becomes

$$\bar{u}\frac{\partial T}{\partial \bar{x}} + \bar{v}\frac{\partial T}{\partial \bar{y}} = \frac{k}{\rho C_p}\frac{\partial^2 T}{\partial \bar{y}^2} + \frac{16}{3\rho C_p k^*}\frac{\partial^2 T}{\partial \bar{y}^2} \;. \quad (5)$$

The appropriate boundary conditions for the problem are given by

$$u = 0, v = 0, T = T_w \;\; at \;\; y = 0, \quad (6)$$

$$\bar{u} \to \bar{u}_e(\bar{x}),\; T \to T_\infty \;\; as \;\; \bar{y} \to \infty \;. \quad (7)$$

Introducing

$$x = \frac{\bar{x}}{L}, \qquad y = Re_L^{\frac{1}{2}}\,\frac{\bar{y}}{L}\,, \qquad u = \frac{\bar{u}}{U_\infty}\;, \quad (8)$$

$$v = Re_L^{\frac{1}{2}}\;\frac{\bar{v}}{U_\infty}\,,\;\; u_e = \frac{\bar{u}_e}{U_\infty}\,,\;\; Re_L = \frac{U_\infty L}{\upsilon}. \quad (10)$$

Putting these values in equations (1), (2) and (5), we get

$$\frac{\partial u}{\partial x}+\frac{\partial v}{\partial y}=0, \tag{11}$$

$$u\frac{\partial u}{\partial x}+v\frac{\partial u}{\partial y}=u_e\frac{\partial u_e}{\partial x}+\frac{1}{\mu^*}\frac{\partial \mu}{\partial T}\frac{\partial T}{\partial y}\frac{\partial u}{\partial y}+\frac{\mu}{\mu^*}\frac{\partial^2 u}{\partial y^2}-\left(\frac{\mu'}{\rho k}.\frac{L}{U_\infty}\right)u \quad -M^2 u, \tag{12}$$

$$u\frac{\partial T}{\partial x}+v\frac{\partial T}{\partial y}=\frac{k}{\upsilon\,\rho C_p}\frac{\partial^2 T}{\partial y^2}+\frac{16\sigma}{3\upsilon\,\rho C_p k^*}\frac{\partial^2 T}{\partial y^2}\ , \tag{13}$$

where $\mu^*=\upsilon\rho$, $M^2=\frac{\sigma_e B_0^2 L}{\rho U_\infty}$, M is Hartmann Number,

Velocity of fluid over wedge is now given by $u_e(x)=x^m\ ,\ for\ m\leq 1.$

Now we introduce the following relations for u, v and θ as

$$u=\frac{\partial \psi}{\partial y}\ ,\ \ v=-\frac{\partial \psi}{\partial x}\quad and \quad \theta=\frac{T-T_\infty}{T_w-T_\infty}. \tag{14}$$

We use the temperature dependent fluid viscosity.

$$\mu=[a+b(T_w-T)=[a+A(1-\theta)], \tag{15}$$

where a, b are constants and $b>0,\ \ A=b(T_w-T_\infty)$

Now using equation (14) and (15) in the boundary layer problem equation (12) and in the energy equation (13), we get the following equations

$$\frac{\partial \psi}{\partial y}\frac{\partial^2 \psi}{\partial x\partial y}-\frac{\partial \psi}{\partial x}\frac{\partial^2 \psi}{\partial y^2}=u_e\frac{\partial u_e}{\partial x}+A\frac{\partial \theta}{\partial y}\frac{\partial^2 \psi}{\partial y^2}+[a+A(1-\theta)]\ \frac{\partial^3 \psi}{\partial y^3}-\sigma^2\ \frac{\partial \psi}{\partial y}\quad -M^2\ \frac{\partial \psi}{\partial y}, \tag{16}$$

$$\frac{\partial \psi}{\partial y}\frac{\partial \theta}{\partial x}-\frac{\partial \psi}{\partial x}\frac{\partial \theta}{\partial y}=\left(\frac{k}{\upsilon\,\rho C_p}+\frac{16\sigma}{3\upsilon\,\rho C_p k^*}\right)\frac{\partial^2 \theta}{\partial y^2}\ , \tag{17}$$

where, $\sigma^2=\left(\frac{\mu'}{\rho k}.\frac{L}{U_\infty}\right)$, σ is the porous parameter, $A=b(T_w-T_\infty)$, the boundary conditions equation (6), (7) reduced

$$\frac{\partial \psi}{\partial y}=0,\qquad \frac{\partial \psi}{\partial x}=0,\qquad \theta=1\quad at \quad y=0. \tag{19}$$

$$\frac{\partial \psi}{\partial y}\to u_e(x)=x^m\ ,\qquad \theta\to 0\qquad as\quad y\to\infty. \tag{20}$$

We introduce the following relations

$$\psi(x,y)=x^\alpha f(\lambda),\qquad \theta(x,y)=G(\lambda),\qquad \lambda=\frac{y}{x^\gamma}\ , \tag{21}$$

Putting these values in the momentum and energy equations, then momentum and energy equations give $\alpha=1-\gamma$ and the momentum equation also gives $\alpha-3\gamma=2m-1$, the solution of which is $\alpha=\frac{1+m}{2},\ \gamma=\frac{1-m}{2}$ and the resulting governing equations then becomes

$$m\,f'^2-\frac{m+1}{2}\,f\,f''=m-AG'f''+[(a+A)-G]\,f''f'''-\sigma^2F'-M^2F', \tag{22}$$

$$(3+4Q)G''+\frac{3}{2}(m+1)\,\mathrm{Pr}\,F\ \ G'+3\,\gamma\,\lambda\,\mathrm{Pr}\,F'\,G'=0, \tag{23}$$

where $Pr=\mu^*C_p/k$ is the Prandtl number, $Q=4\sigma_s\,T_\infty^3/kk^*$ is the radiative heating parameter.

The boundary conditions take the following form

$$F'=0, F=0, G=1\ at\ \lambda=0\quad , \tag{24}$$

$and\ F' \to 1, G \to 0\ \ as\ \ \lambda \to \infty$. (25)

Using the boundary condition (24) in equation (25), we get

$$(3+4Q)G'' + \frac{3}{2}(m+1)\,\mathrm{Pr}\,F\ G' = 0. \quad (26)$$

Here the above differential equation (26), $Pr = \mu^* C_p / k$ is the Prandtl number, $Q = 4\sigma_s T_\infty^3 / kk^*$ is the radiative heating parameter.

Solving the above equation (26), using the boundary conditions (24) and (25), we get

$$G = e^{-\frac{3}{2}\frac{(m+1)}{(3+4Q)}\,Pr\,F\,\lambda} \quad . \quad (27)$$

Now solving the above differential equation (22) & (27) numerically by using ode45 solver in MATLAB software.

3. METHOD OF SOLUTION

We have solved the above differential equations (22), (23) & (27) numerically using MATLAB software with the help of ode45 solver. The set of differential equations with described boundary conditions. For the purpose the time interval (0, 10) with initial condition vector (0, 0, 1) has been taken for convergence criteria. The option has been chosen ('RelTol', 1e-4,'AbsTol', [1e-4 1e-4 1e-5]). The different set of parameter has been chosen to investigate the results. The range of dimensionless variable $\lambda(\,0 \le \lambda \le 10)$, the value of Magnetic Parameter M has taken (1, 2, 3, 4, 5), Radiative heating parameter Q (1, 2, 3, 4, 5), Prandtl number Pr {1, 2, 3, 4, 5}, Falkner-Skan exponent parameter m has been taken {0.1, 0.3, 0.5, 0.7, 0.9}, temperature-dependent viscosity parameter A (5, 10, 20, 30, 40), Porous wedge parameter σ has been taken {1, 2, 3, 4, 5}, etc.,. The various graphs have been plotted with described set of parameters and discussed in detail in the next section.

4. RESULTS AND DISCUSSION

In this paper we have to investigate numerical method and has been carried out for various values of the Magnetic Parameter M, Porous wedge parameter σ, temperature-dependent viscosity parameter (A), Falkner-Skan exponent (m), Radiative heating parameter (Q) and Prandtl Number Pr. For illustrations of the results, numerical values are plotted in the below figures. From fig. 1, 2, 3 and 4 is the graphs between axial velocity $f(\lambda)$ and radial velocity $f'(\lambda)$ of fluid against dimensionless variables λ, at different constants parameters; it is seen that axial and radial velocity of fluids sharply increases with enhancement of magnetic parameter M and porous wedge parameter σ. Figure 5, 6, 9 & 10 represented as the axial velocity $f(\lambda)$ and radial velocity $f'(\lambda)$ of fluid against dimensionless variable λ, at different constants parameters; it is seen that axial and radial velocity component of fluid sharply decreases with increase temperature dependent viscosity parameter A. Figures 7 & 8 represented as the axial velocity $f(\lambda)$ and radial velocity $f'(\lambda)$ of fluid against dimensionless variable λ, at different constants parameters; it is found that that axial and radial velocity component of fluid sharply decreases with decrease Falkner Skan exponent m.

Figure 11, 12, 13 & 14 represents Heat components of fluids $G(\lambda)$ against dimensionless variable λ, at different constants variables; it is found that heat components of fluids decreases sharply with increase of Magnetic parameter M, Porous parameter σ, Radiative heating parameter Q and Prandtl number Pr. Figure 15 is the graph of heat components of fluids $G'(\lambda)$ against dimensionless variable λ, at different constants variables; it is obtained that heat components of fluids decreases with increase of Radiative heating parameter Q. Figure 16 is graph between heat components of fluids $G'(\lambda)$ against dimensionless variable λ, at different constants variables; it is obtained that heat flow of fluids increases slowly with increase of magnetic parameter M. Figure 17 is graph between heat components of fluids $G'(\lambda)$ against dimensionless variable λ, at different constants variables; it is found that heat flow of fluids increases slowly with increase of Prandtl number Pr. Figure 18 is graph between heat components of fluids $G(\lambda)$ against dimensionless variable λ, at different constants parameter; it is found that heat flow of fluids decreases sharply with increase of Falkner Skan exponent m. Figure 19 is graph between heat components of fluids $G'(\lambda)$ against dimensionless variable λ, at different constants parameter; it is found that heat flow of fluids increases slowly with increase of Falkner Skan exponent m.

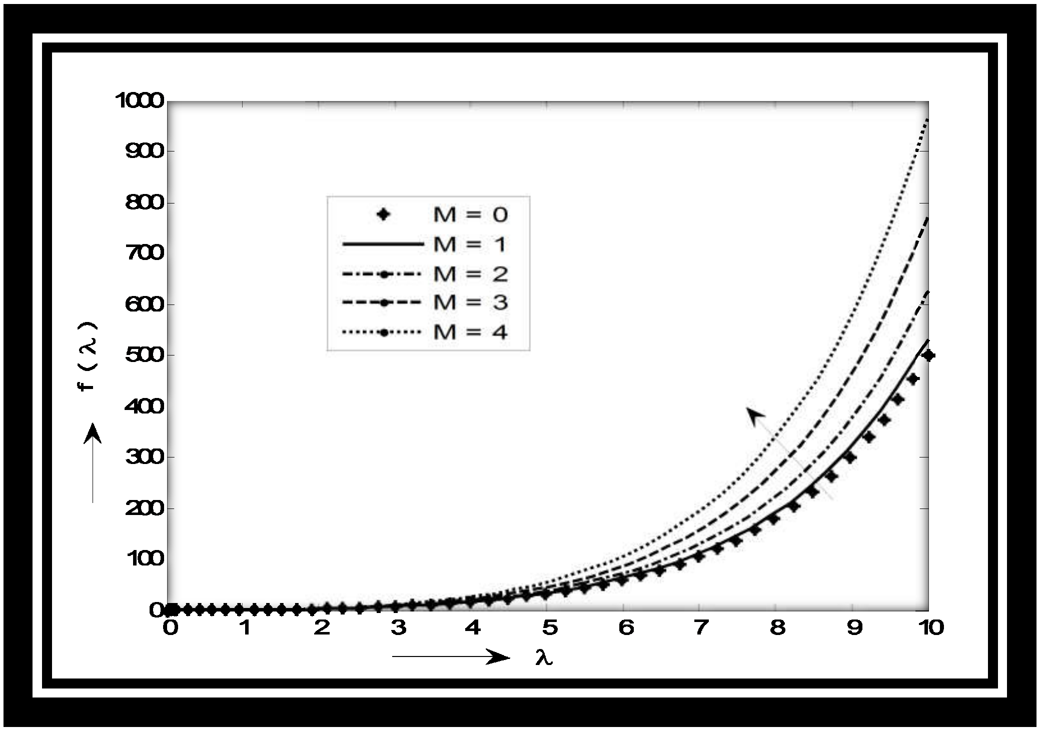

Fig 1. Graph between axial velocity component of fluid $f(\lambda)$against dimensionless variable λ with variation of Magnetic parameter M (0, 1, 2, 3, 4) at constant parameters m = 0.5, a = 2, Q = 2, A = 10, Pr = 0.5 and σ = 2.

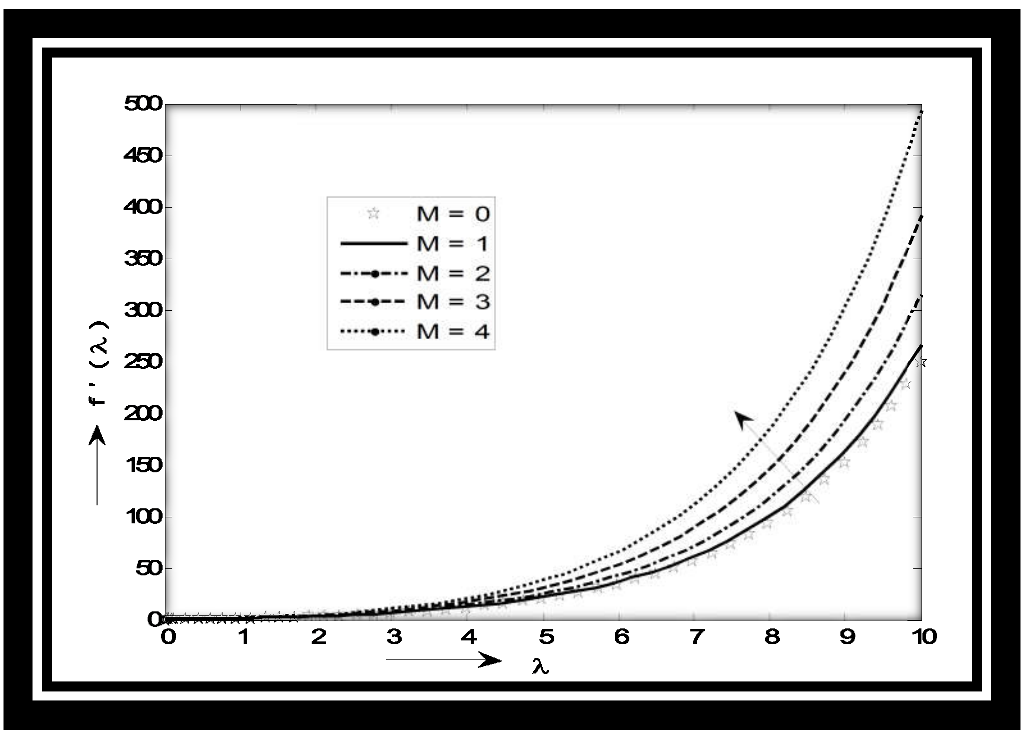

Fig 2. Graph between radial velocity component of fluid $f'(\lambda)$against dimensionless variable λ with variation of Magnetic parameter M (0, 1, 2, 3, 4) at constant parameters m = 0.5, a = 2, Q = 2, A = 10, Pr = 0.5 and σ = 2.

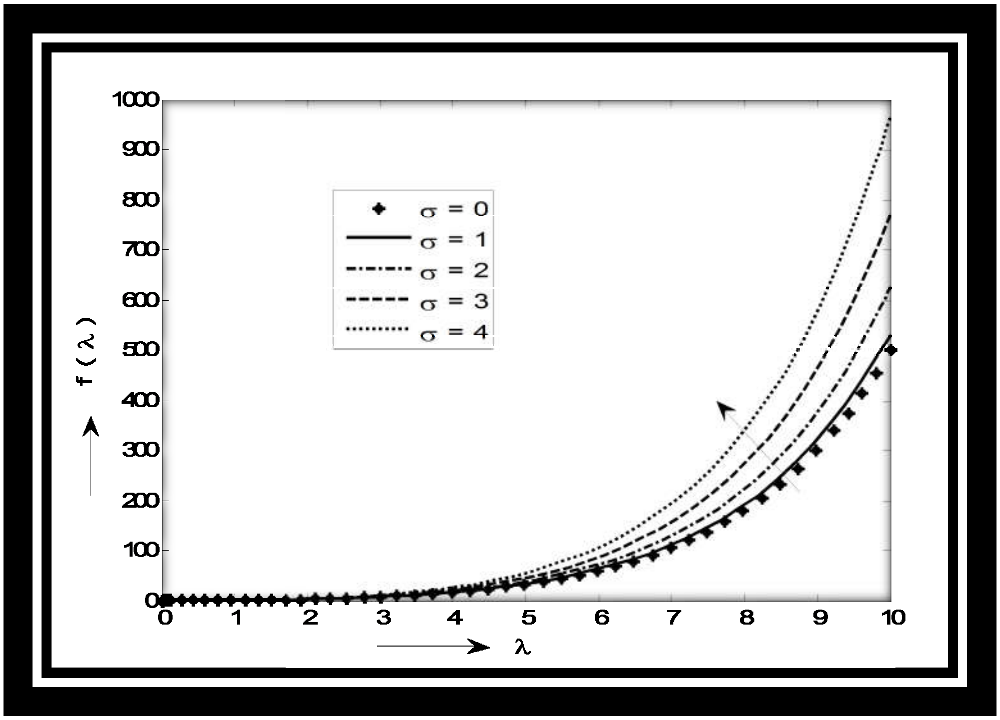

Fig 3. Graph between axial velocity component of fluid $f(\lambda)$against dimensionless variable λ with variation of porous wedge parameter σ (0, 1, 2, 3, 4) at constant parameters m = 0.5, a = 2, Q = 2, A = 10, Pr = 0.5 and M = 2.

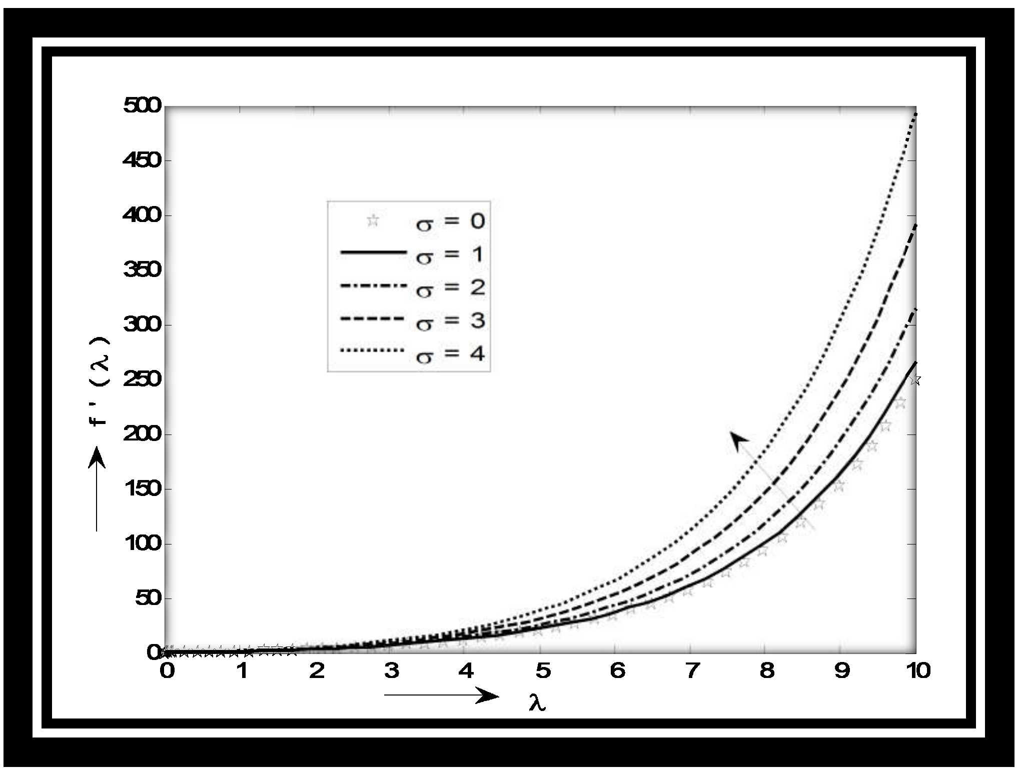

Fig 4. Graph between radial velocity component of fluid $f'(\lambda)$against dimensionless variable λ with variation of porous wedge parameter σ (0, 1, 2, 3, 4) at constant parameters m = 0.5, a = 2, Q = 2, A = 10, Pr = 0.5 and M = 2.

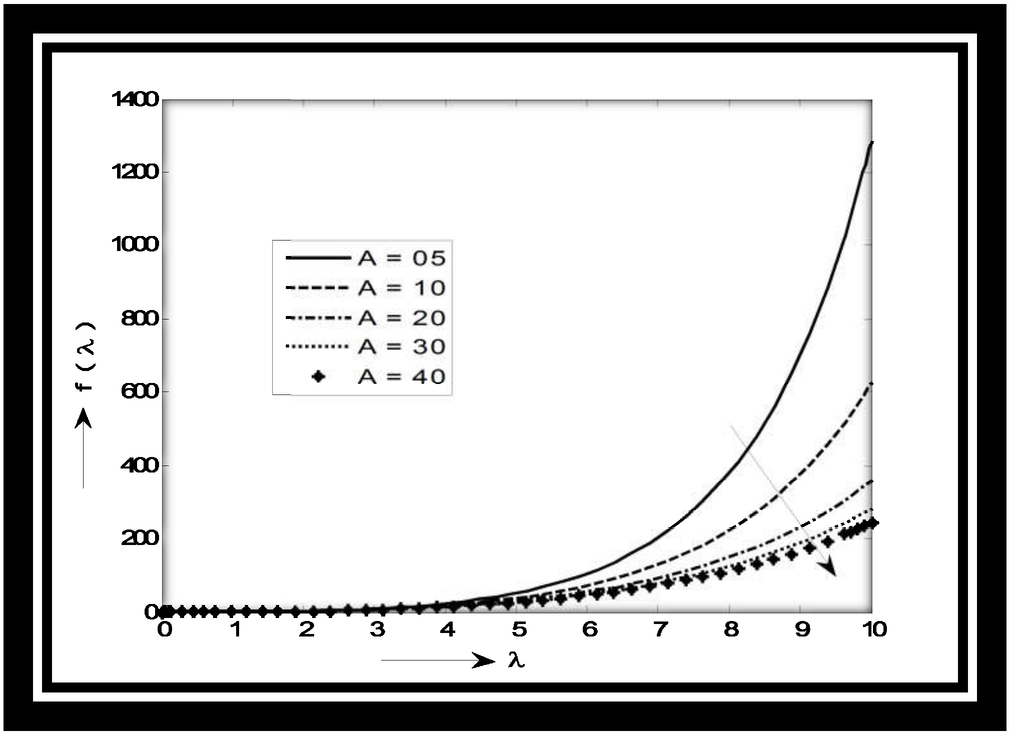

Fig 5. Graph between axial velocity component of fluid $f(\lambda)$against dimensionless variable λ with variation of Temperature dependent viscosity parameter A (5, 10, 02, 30, 40) at constant parameters m = 0.5, a = 2, Q = 2, σ = 2, Pr = 0.5 and M = 2.

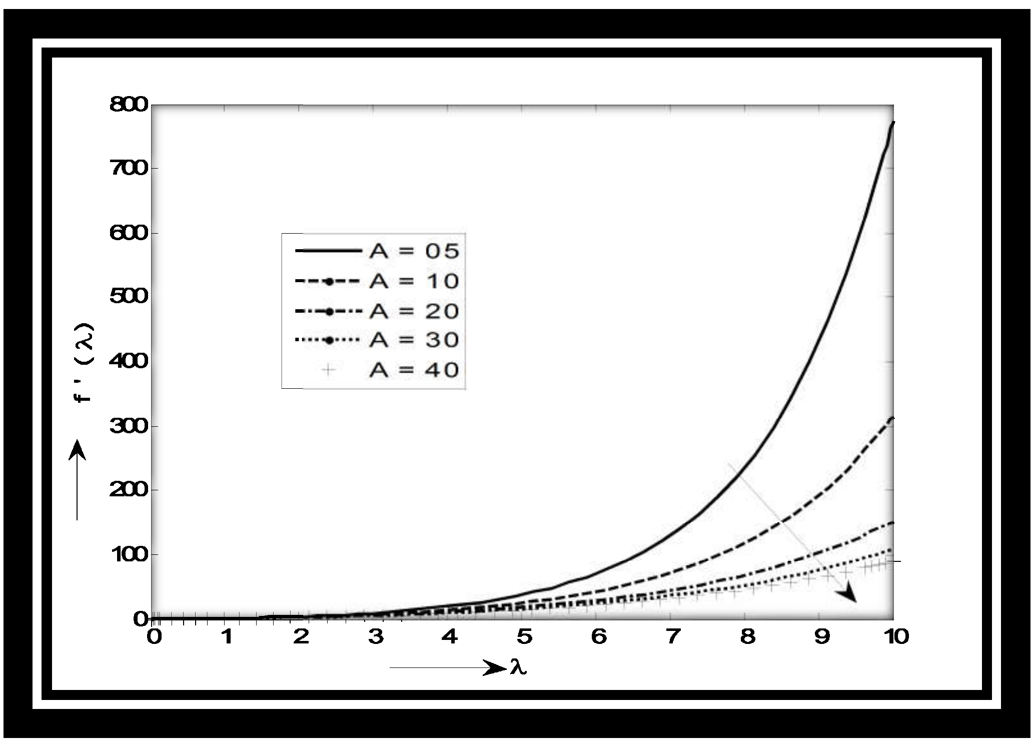

Fig 6. Graph between radial velocity component of fluid $f'(\lambda)$against dimensionless variable λ with variation of Temperature dependent viscosity parameter A (5, 10, 02, 30, 40) at constant parameters m = 0.5, a = 2, Q = 2, σ = 2, Pr = 0.5 and M = 2.

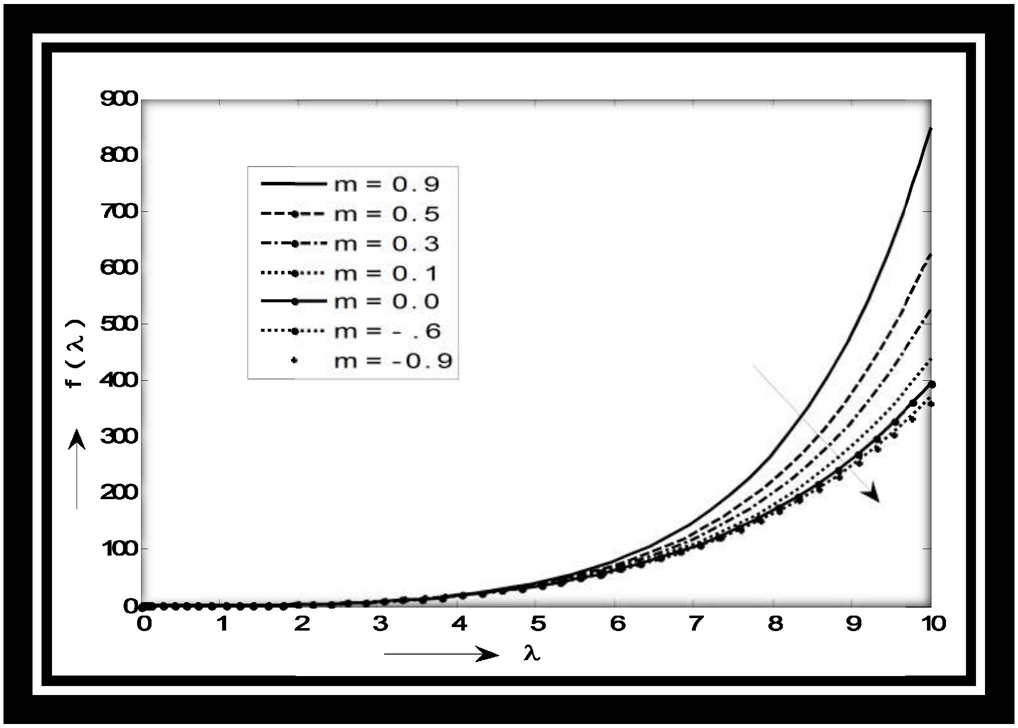

Fig 7. Graph between axial velocity component of fluid $f(\lambda)$against dimensionless variable λ with variation of Falkner Skan Exponent parameter m (0.9, 0.5, 0.3, 0.1, 0.0, - 0.06, - 0. 09) at constant parameters A = 10, a = 2, Q = 2, σ = 2, Pr = 0.5 and M = 2.

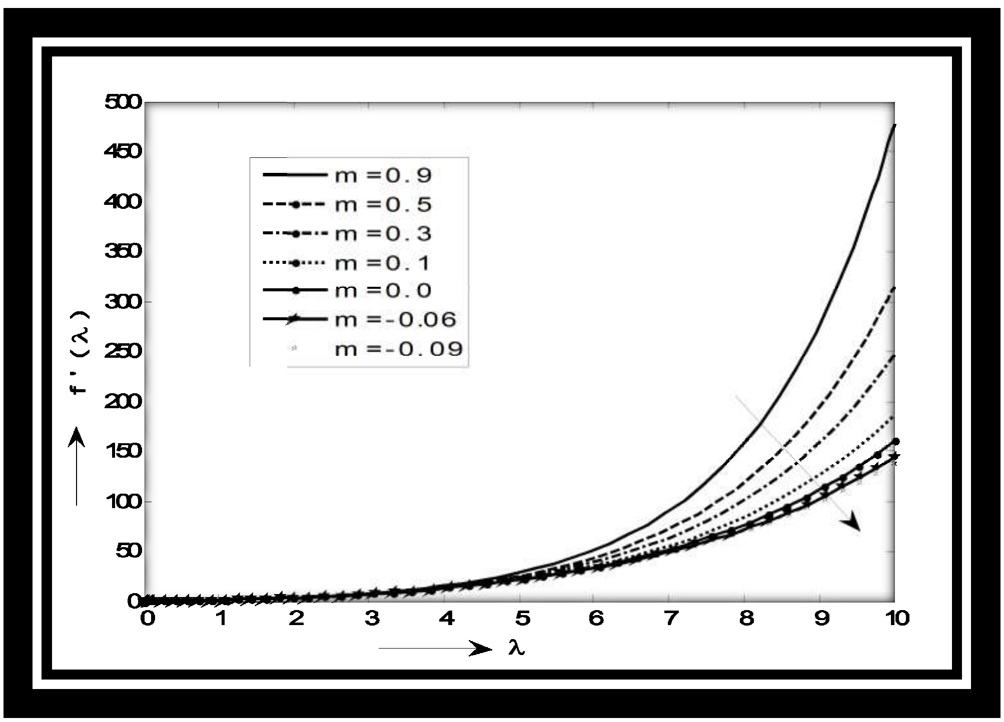

Fig 8. Graph between radial velocity component of fluid $f'(\lambda)$against dimensionless variable λ with variation of Falkner Skan Exponents parameter m (0.9, 0.5, 0.3, 0.1, 0.0, - 0.06, - 0. 09) at constant parameters A = 10, a = 2, Q = 2, σ = 2, Pr = 0.5 and M = 2.

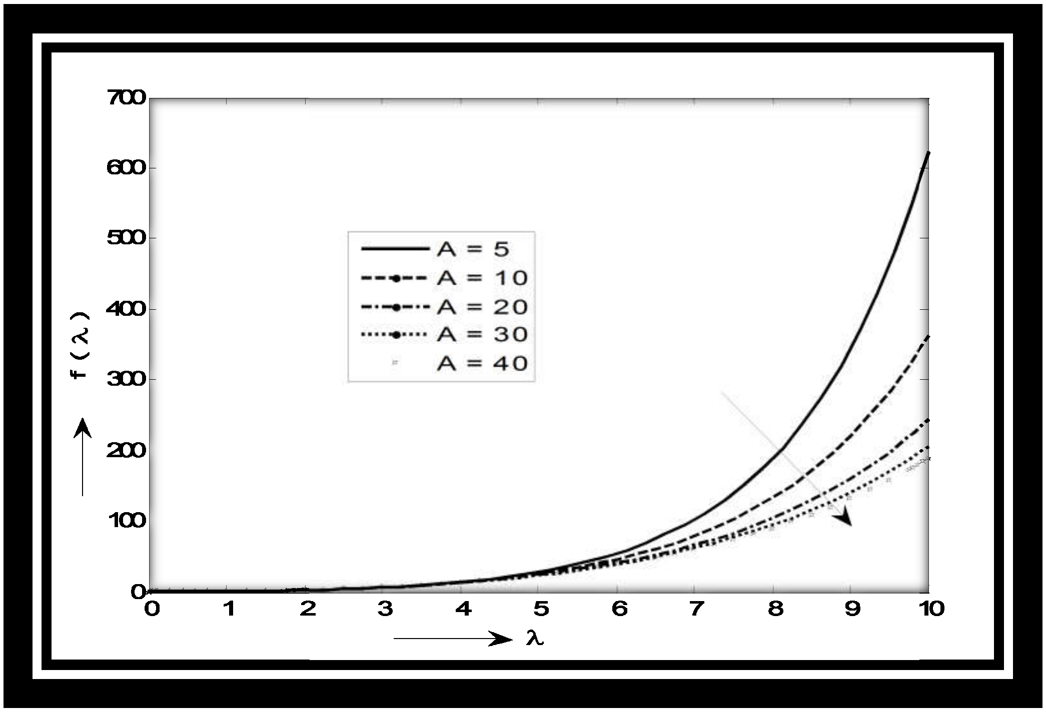

Fig 9. Graph between axial velocity component of fluid $f(\lambda)$against dimensionless variable λ with variation of Temperature dependent viscosity parameter A (5, 10, 20, 30, 40) at constant parameters m = 0.5, a = 2, Q = 2, σ = 2, Pr = 0.5 and M = 0.

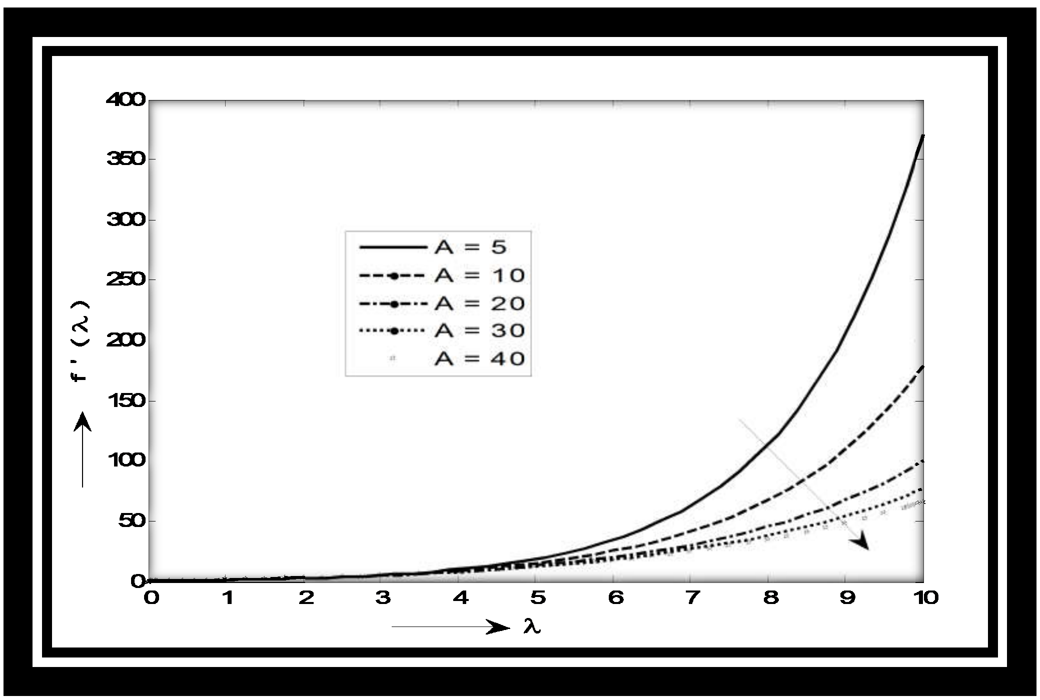

Fig 10. Graph between radial velocity component of fluid $f'(\lambda)$against dimensionless variable λ with variation of Temperature dependent viscosity parameter A (5, 10, 20, 30, 40) at constant parameters m = 0.5, a = 2, Q = 2, σ = 2, Pr = 0.5 and M = 0.

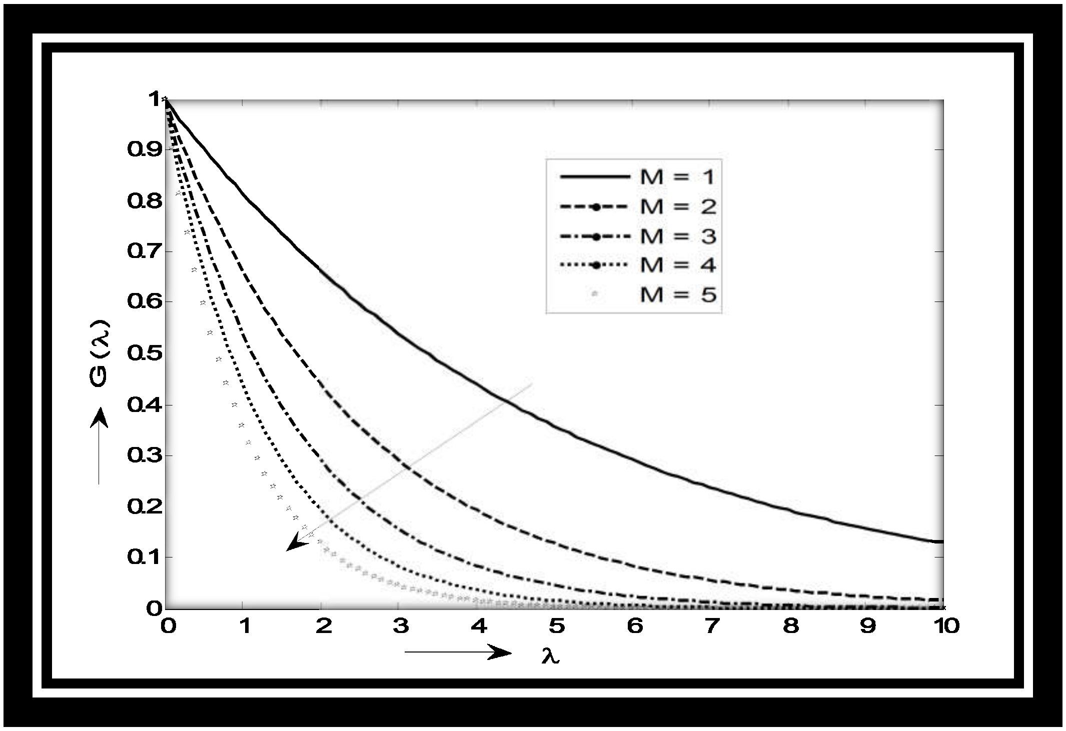

Fig 11. Graph between heat flow of fluid $G(\lambda)$against dimensionless variable λ with variation of Magnetic parameter M (1, 2, 3, 4, 5) at constant parameters m = 0.5, a = 2, Q = 2, σ = 2, Pr = 0.5 and A =1 0.

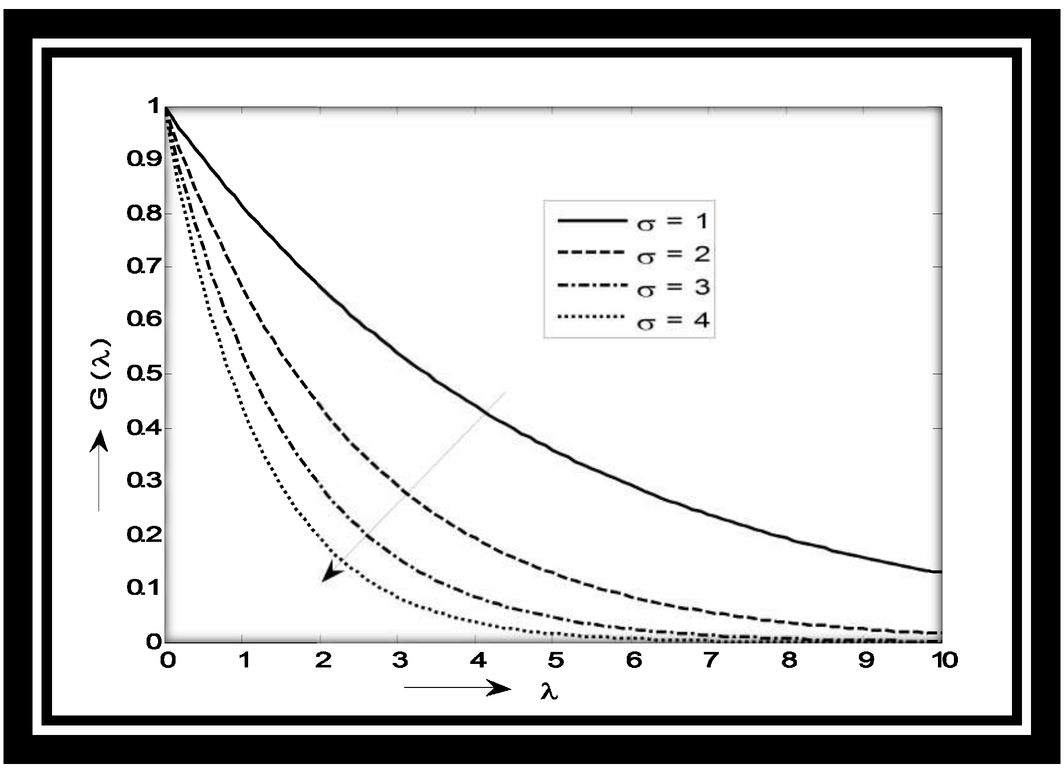

Fig 12. Graph between heat flow of fluid $G(\lambda)$against dimensionless variable λ with variation of porous wedge parameter σ (1, 2, 3, 4) at constant parameters m = 0.5, a = 2, Q = 2, M = 2, Pr = 0.5 and A =1 0.

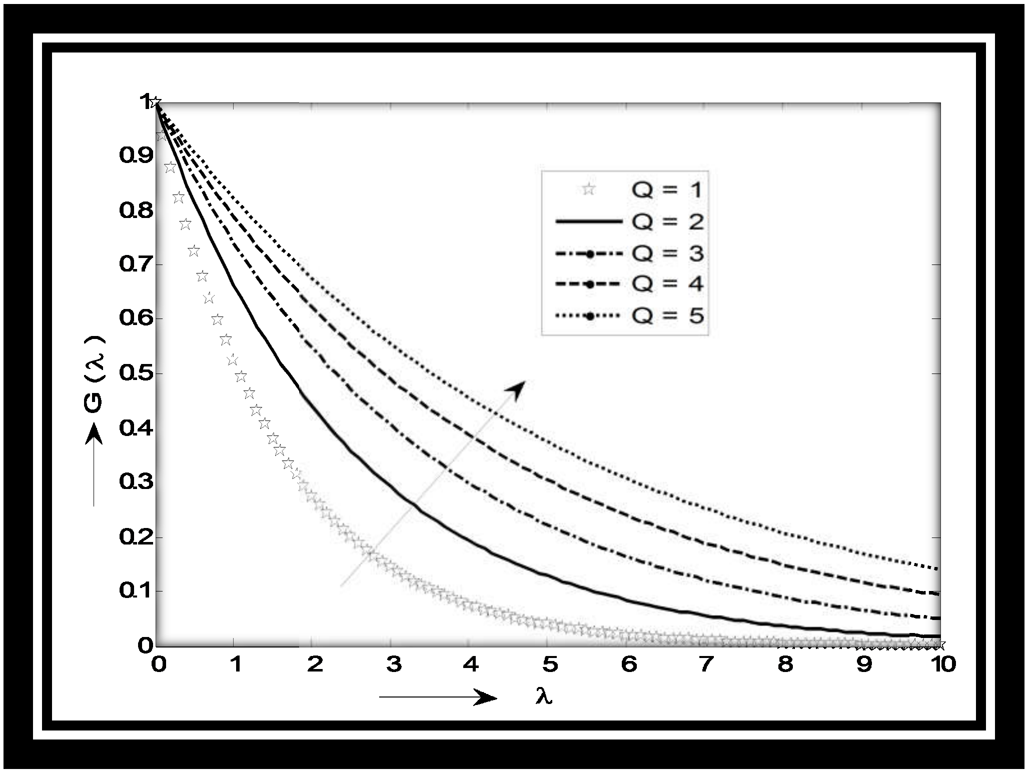

Fig 13. Graph between heat flow of fluid $G(\lambda)$against dimensionless variable λ with variation of Radiative heating parameter Q (1, 2, 3, 4, 5) at constant parameters m = 0.5, a = 2, σ = 2, M = 2, Pr = 0.5 and A =1 0.

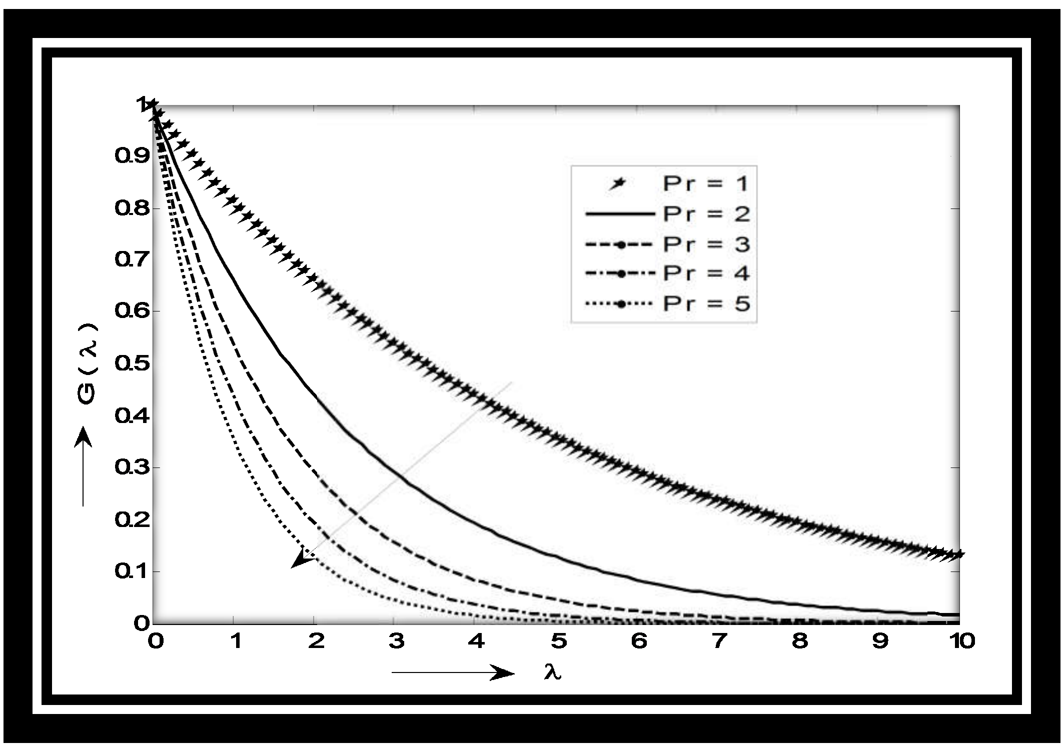

Fig 14. Graph between heat flow of fluid $G(\lambda)$against dimensionless variable λ with variation of Prandtl number Pr (1, 2, 3, 4, 5) at constant parameters m = 0.5, a = 2, σ = 2, M = 2, Q = 2 and A =1 0.

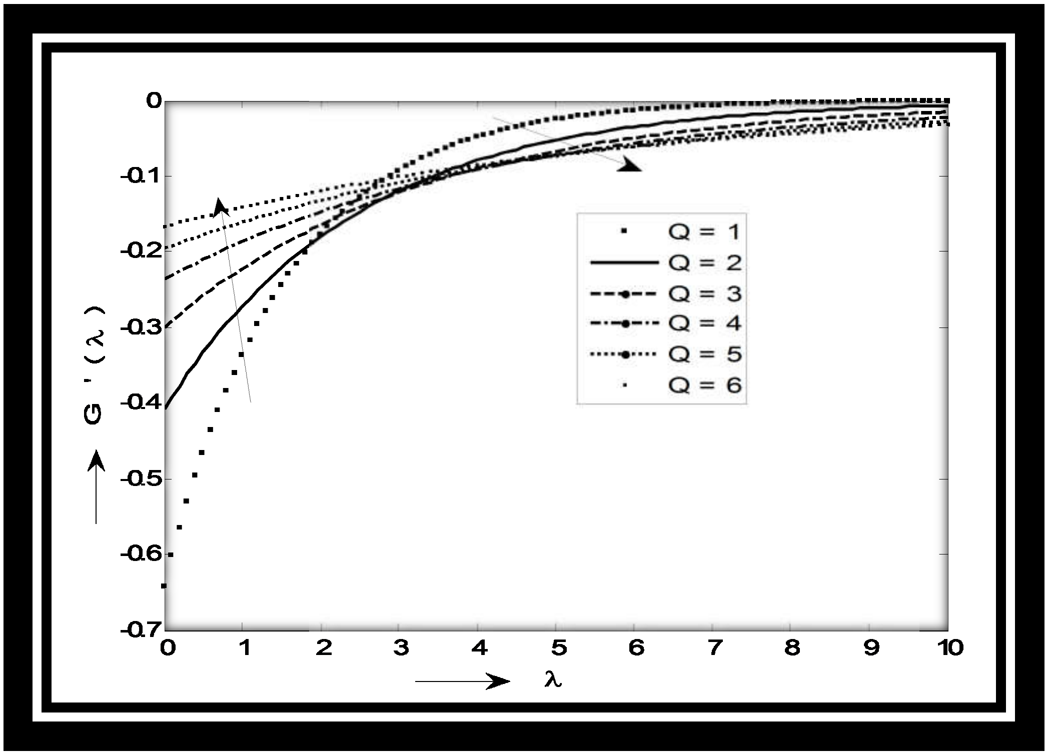

Fig 15. Graph between heat flow of fluid $G'(\lambda)$against dimensionless variable λ with variation of Radiative heating parameter Q (1, 2, 3, 4, 5, 6) at constant parameters m = 0.5, a = 2, σ = 2, M = 2, Pr = 0.5 and A =10.

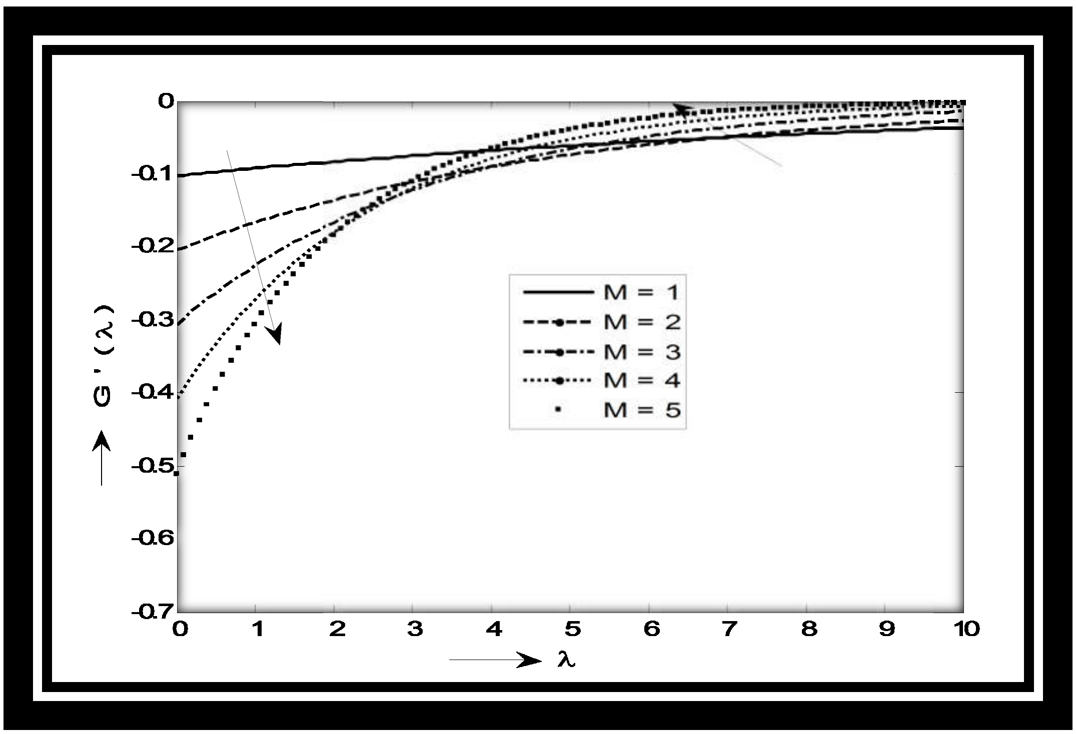

Fig 16. Graph between heat flow of fluid $G'(\lambda)$against dimensionless variable λ with variation of Magnetic parameter M (1, 2, 3, 4, 5) at constant parameters m = 0.5, a = 2, σ = 2, Q = 2, Pr = 0.5 and A =1 0.

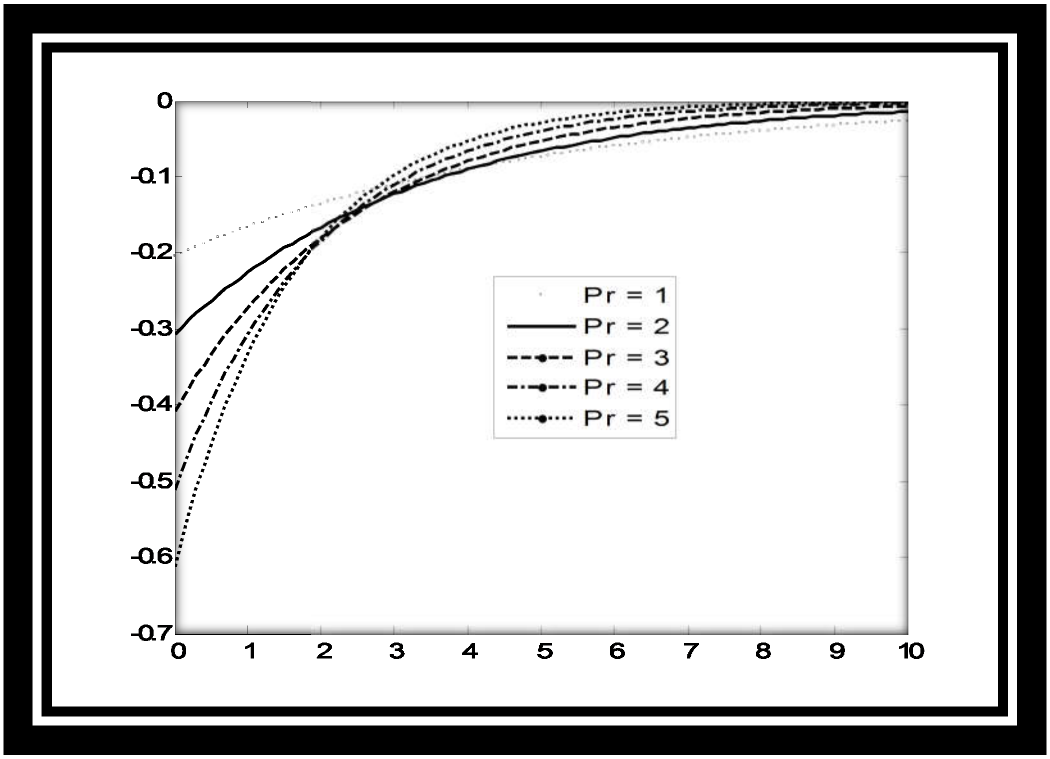

Fig 17. Graph between heat flow of fluid $G'(\lambda)$against dimensionless variable λ with variation of Prandtl number Pr (1, 2, 3, 4, 5) at constant parameters m = 0.5, a = 2, σ = 2, M = 2, Q = 2 and A =1 0.

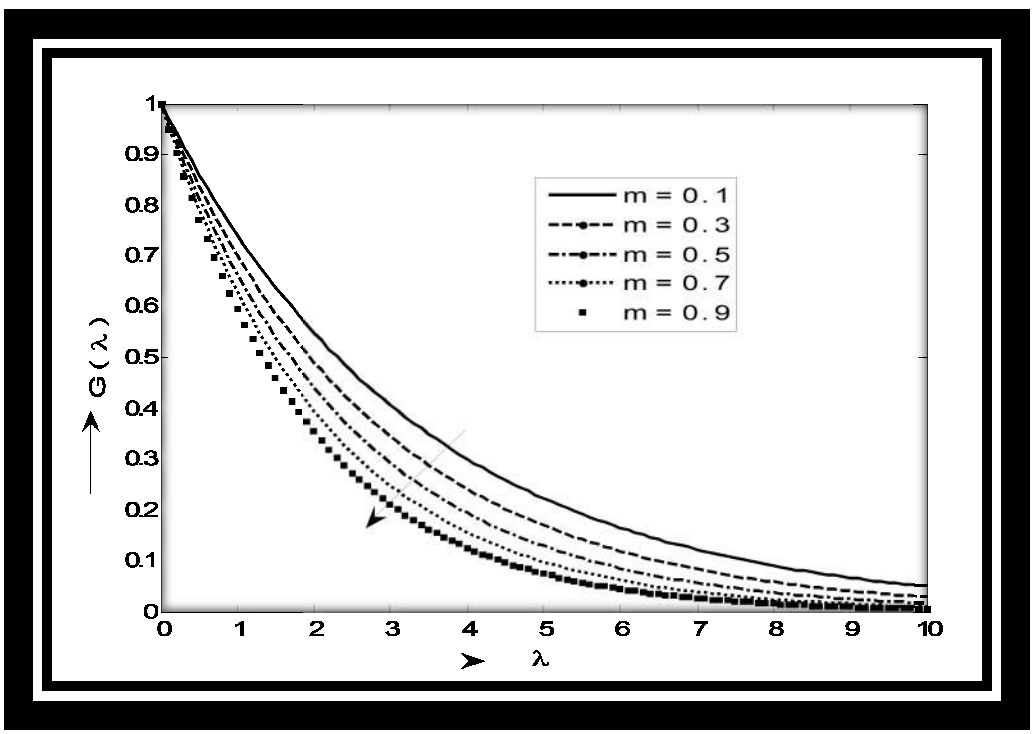

Fig 18. Graph between heat flow of fluid $G(\lambda)$against dimensionless variable λ with variation of Falkner Skan exponent m (0.1, 0.3, 0.5, 0.7, 0.9) at constant parameters Q = 2, a = 2, σ = 2, M = 2, Pr = 0.5 and A =1 0.

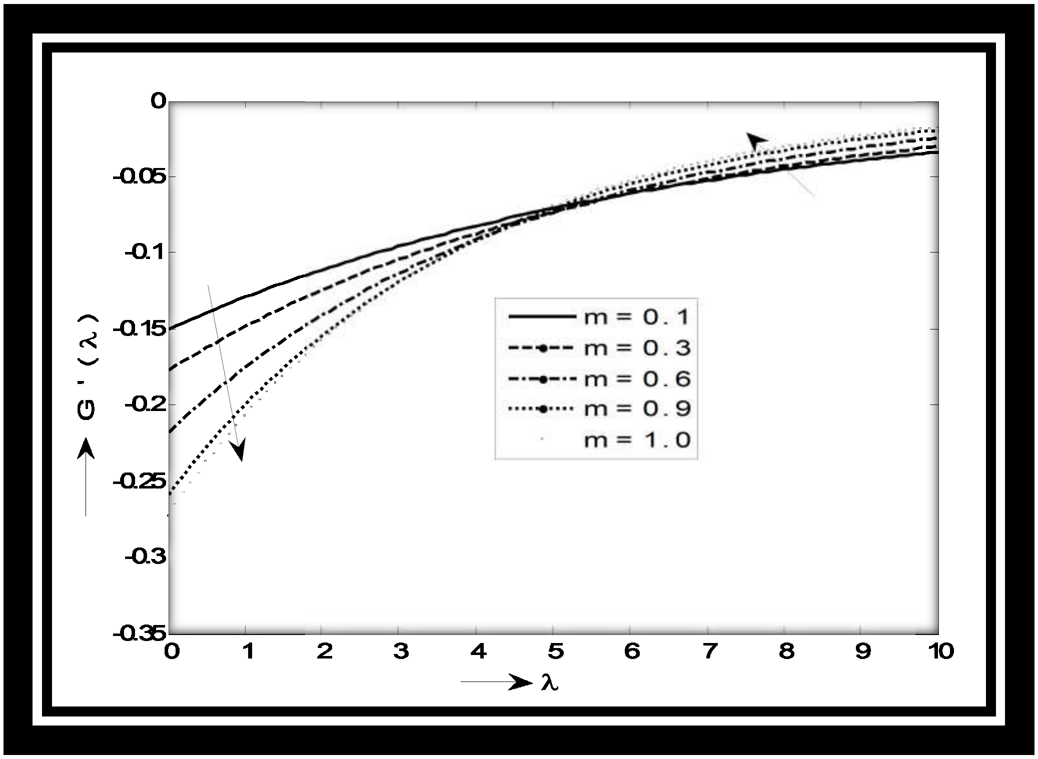

Fig 19. Graph between heat transfer of fluid $G'(\lambda)$ against dimensionless variable λ with variation of Falkner Exponent m (0.1, 0.3, 0.5, 0.7, 0.9) at constant parameters Q = 2, a = 2, σ = 2, M = 2, Pr = 0.5 and A =1 0.

5. CONCLUSIONS

In this present study gives numerical investigation of magneto hydro dynamic flow with variable fluid viscosity and heat transfer in symmetrical sharp porous wedge. The main objective is to analyze the affects of Magnetic parameter M, porous wedge parameter, Prandtl number Pr and Temperature dependent viscosity parameter A on radial and axial velocity components of fluids and heat transfer. We have seen that enhancement of magnetic parameter M and porous wedge parameter σ, radial and axial velocity component of fluid sharply increases, and reciprocal affects with increase of temperature dependent viscosity parameter A, Falkner skan exponent m on fluid velocity components. The heat transfer components of fluid decreases sharply with increases of Falkner skan exponent m, magnetic parameter M, porous wedge parameter σ and Prandtl number Pr whereas increase of radiative heating parameter Q, heat transfer increases sharply. The important application of this problem is linked in engineering and post accidental heat removal. The results of this analysis have been obtained on focusing on magnetic factor and Prandtl number.

REFERENCES:

[1]. D. D. Ganji and A. Rajabi., (2006); 'Assessment of homotopy-perturbation and perturbation methods in heat radiation equations.' International communications in heat and mass transfer, Vol. 33, No. 3, pp. 391 – 400.

[2]. H. C. Suratiand and M. G. Timol., (2010); 'Numerical study of forced convection wedge flow of some non-Newtonian fluids.' International Journal of Applied Mathematics and Mechanics, Vol. 6, No. 18, pp. 50 – 65.

[3]. M. A. Hossain, M. S. Munir and D. A. S. Rees., (2000); 'Flow of viscous incompressible fluid with temperature dependent viscosity and thermal conductivity past a permeable wedge with uniform surface heat slux.' International Journal of Thermal sciences, Vol. 39, pp. 635 – 644.

[4]. M. B. Abd-el-Malek, N. A. Badran and H. S. Hassan., (2002); 'Solution of the Rayleigh problem for a power law non-Newtonian conducting fluid via group method.' Int. Jour Eng. Sci. Vol. 40, pp. 1599 – 1609.

[5]. M. A. Hossain, S. Bhowmik and R. S. R. Gorla., (2006); 'Unsteady mixed-convection boundary layer flow along a symmetric wedge with variable surface temperature.' International Journal of Engineering Science, Vol. 44, pp. 607 – 620.

[6]. Navneet Kumar Singh and Ramesh Yadav (2017); 'Investigation of heat transfer of non-Newtonian fluid in the presence of a porous wall.' International Journal of Engineering Technologies and Management Research (IJETMR), Vol. 4, Issue 12, pp. 74 – 92.

[7]. P. G. Daniels.,(2007); 'On the boundary layer structure of differentially heated cavity flow in a stably stratified porous medium.' Jour. Fluid Mech, Vol. 586, pp 347 – 370.

[8]. Ramesh Yadav and Navneet Kumar Singh (2017); 'Analytical investigation of thermal radiation effects on laminar flow of fluid and heat transfer in a channel with two porous bounding walls on different permeability.' Applied Research Journal, Vol. 3, Issue 7, pp. 216 – 230.

[9]. Ramesh Yadav, Manju Agarwal and Vivek Joseph., (2016); 'Investigation of laminar flow of fluid with one porous bounding wall." Int. Jour. of Science and Research (IJSR), Vol. 5, Issue 1. pp. 261 – 267.

[10]. Ramesh Yadav and Vivek Joseph., (2016); 'Numerical analysis of MHD flow of fluid with one porous bounding wall.' International Research Journal of Engineering and Technology (IRJET), Vol. 03, Issue 02, pp. 726 – 737.

[11]. S. Mukhopadhyay., (2009); 'Effect of radiation and variable fluid viscosity on flow and heat transfer along a symmetric wedge.' Journal of Applied Fluid Mechanics, Vol. 2, No. 2, pp. 29 – 34.